



ORIGINAL ARTICLE

Design and synthesis of chitosan/agar/Ag NPs: A potent and green bio-nanocomposite for the treatment of glucocorticoid induced osteoporosis in rats



Dongliang Shi^{a,b}, Bikash Karmakar^{c,*}, Hosam-Eldin Hussein Osman^d,
Attalla F. El-kott^{e,f}, Kareem Morsy^{e,g}, Mohamed M. Abdel-Daim^{h,i}

^a Henan University of Traditional Chinese Medicine, Zhengzhou 450046, China

^b Orthopedics Dept.1, Henan Hospital of Traditional Chinese Medicine (The Second Affiliated Hospital of Henan University of Chinese Medicine), Zhengzhou 450002, China

^c Department of Chemistry, Gobardanga Hindu College, India

^d Anatomy Department, College of Medicine, Taif University, P.O. Box 11099, Taif 21944, Saudi Arabia

^e Biology Department, College of Science, King Khalid University, Abha 61421, Saudi Arabia

^f Zoology Department, College of Science, Damanhour University, Damanhour 22511, Egypt

^g Department of Zoology, Faculty of Science, Cairo University, Cairo, Egypt

^h Pharmaceutical Sciences Department, Pharmacy Program, Batterjee Medical College, P.O. Box 6231, Jeddah 21442, Saudi Arabia

ⁱ Pharmacology Department, Faculty of Veterinary Medicine, Suez Canal University, Ismailia 41522, Egypt

Received 13 June 2021; accepted 29 September 2021

Available online 8 October 2021

KEYWORDS

Chitosan-agar;
Silver nanoparticles;
Osteoporosis;
Glucocorticoid;
Rat

Abstract In this work we have demonstrated the green synthesis of stable and mono-dispersed Ag NPs using chitosan/Agar hydrogel having reducing/stabilizing ability avoiding any toxic reagents. Agarose was used as a green reductant for the synthesis of Ag NPs which gets stabilized by chitosan. The *in situ* prepared Ag NPs@CS/Agar nano bio-composite were characterized by advanced physicochemical techniques like Fourier Transformed Infrared spectroscopy (FT-IR), Scanning Electron Microscopy (SEM), Transmission Electron Microscopy (TEM), Energy Dispersive X-ray spectroscopy (EDX) and X-ray Diffraction (XRD) study. The Ag NPs encapsulated by CS/Agar bio-composite have a spherical shape with a mean diameter from 10 to 15 nm. Towards its bioapplication, the Ag NPs@CS/Agar nano bio-composite was administered by 5 µg/kg/day for 30 days in comparison to methyl prednisolone sodium succinate by 10 mg/kg, sc, thrice a week for

* Corresponding author.

E-mail address: bkarmakar@ghcollege.ac.in (B. Karmakar).

Peer review under responsibility of King Saud University.



4 weeks over Wistar rats having glucocorticoid induced osteoporosis. This showed a significant increase in the serum levels of bone mineral content markers and a decrease in serum and urinary levels of bone resorption markers. An inclination in strength of femur and tibia was seen particularly with 5 µg/kg of Ag NPs@CS/Agar nano bio-composite. Maintenance of calcium homeostasis, formation of collagen and scavenging of free radicals can be the plausible mode of action of this bio-nanocomposite thereby combating osteoporosis induced by glucocorticoids.

© 2021 Published by Elsevier B.V. on behalf of King Saud University. This is an open access article under the CC BY-NC-ND license (<http://creativecommons.org/licenses/by-nc-nd/4.0/>).

1. Introduction

Glucocorticoids are naturally occurring steroid hormones being excreted from the cortex of adrenal gland. They control the essential body functions and have powerful anti-inflammatory properties in animal and human body. It also helps in preventing the rejection of transplanted body parts (Timmersmans et al., 2019). From the last few decades synthetic glucocorticoid drugs are extensively used as immune suppressant for the treatment of allergic diseases, gastrointestinal diseases, rheumatism, systemic lupus erythematosus and also in cancers. However, prolonged intake of these drugs are reported to have severe side-effects. Glucocorticoid induced osteoporosis (GIOP) is one of the major among them, observed mainly in adults (Gudbjornsson et al., 2002; Lin et al., 2014). In healthy adult body, bone is constantly rehabilitated by a synchronized process where osteoclast cells degrade and resorb the old bones, initiates reformation of new bones and simultaneously osteoblast cells take part in skeletal development by redepositing and mineralizing new bone templates (Kanis et al., 2008; Moshiri et al., 2017). Now, a pronounced osteoclast apoptosis makes a disparity in this physiological procedure resulting decreased bone mineral density and corrosion in bone microstructure, usually named as osteoporosis (Mora-Raimundo et al., 2019; Andersen et al., 2013; Ding et al., 2019). Glucocorticoids directly influence the osteoblast activity and indirectly through the inhibition of insulin-like growth factor I expression, which in turn affects the Ca level and sex hormone level of the body (Jia et al., 2011; Ilias et al., 2000; Dushyanthen et al., 2013; Van Staa et al., 2000). The GIOP ultimately causes bones to become fragile, loss of height, severe pains in wrist, knee, spine and hip area and also susceptible to fracture on even minor jerk like sneezing. For the treatment and prevention of GIOP, there are several conventional drugs, viz., the anti-resorptive bisphosphonates (alendronate, risedronate, denosumab, zoledronate) and the recombinant parathyroid hormone, teriparatide (Pizzino et al., 2017). Nevertheless, these pharmacological treatments involve several drawbacks related to toxicity and bioavailability issues. They are not recommended for pregnant or breast-feeding women. They also display a number of side effects like gastrointestinal problems, osteonecrosis of jaws, pain, weakness, heartburn, leg cramps, dizziness, muscle spasm and nausea (Rutkowski, 2011; Khan et al., 2015; Bultink et al., 2013). Therefore, it definitely demands an alternative formulation of novel biocompatible drugs that is free from these issues and exhibits significant bone anabolism.

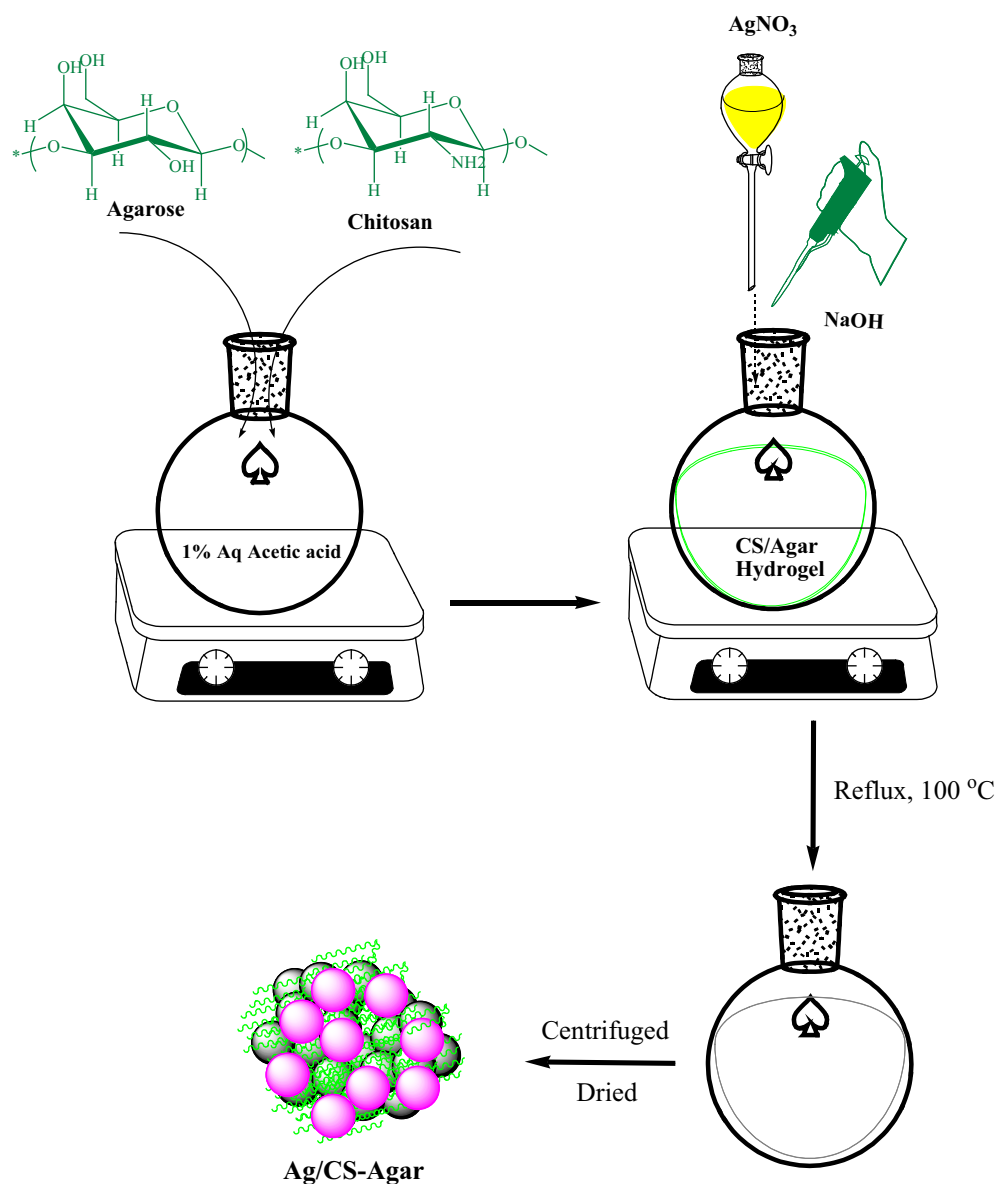
In recent days, biomolecular engineered nanoparticles (NPs) have come into prominence as novel formulated nanomedicine due to their excellent biocompatibility, small size to overcome

the cell barrier, large surface area to carry the effective drug with high loading and selective targeting the drug to the affected area. There are ample reports on plant phytochemicals or biopolymer adorned nanoparticles being deployed in medicinal therapeutics (Xue et al., 2021; Shi et al., 2021; Huang et al., 2021; Zhao et al., 2021; Oueslati et al., 2020; Venditti, 2019; Rossi et al., 2016; Umamaheswari et al., 2018; Fratoddi et al., 2018; Aswathy Aromal and Philip, 2012; Zhang et al., 2020; Entezari et al., 2014; Xu et al., 2021; Ding et al., 2021). Among the different metal variants Ag NPs have been observed to demonstrate significant bioactivities as antioxidant, antifungal and antibacterial properties over diverse fungi and bacteria (Yin et al., 2020; Loo et al., 2018). They have also been explored to have significant potential in cancer diagnosis and also as non-conventional chemotherapeutic drug both *in vitro* and *in vivo* studies (Gomes et al., 2021; Huy et al., 2020; Xu et al., 2020). In the last few years, nanoparticles have been found to be promising carriers for efficient therapeutic delivery in bone disease therapy. For bone regeneration in osteoporosis patients, the development of nanoparticles is ideal since bone itself is a nanocomposite. In addition to this dimensional similarity, they can offer drug protection from biodegradation, transport efficiency, and even improve its pharmacokinetic, pharmacodynamics, biodistribution and targeting (Nluan et al., 2015; Sree et al., 2009; Salamanna et al., 2021; Barry et al., 2016; Raimundo et al., 2017). These inputs have encouraged us to develop a novel nanocomposite material where *in situ* prepared Ag NPs have been embedded over the biocomposite formed with two biomolecules chitosan and agarose (Scheme 1). These hydrogel formed by the two molecules contain plenteous electron rich functional groups which facilitate the green reduction of Ag ions to corresponding NPs without involving toxic chemicals. The bimolecular hydrogel coatings also provide significant stability to the Ag NPs by capping it, thereby preventing from agglomeration. The as-synthesized nanocomposite material has been characterized with different physicochemical techniques and subsequently applied as a chemotherapeutic drug in the detection and treatment of GIOP. This time we took the advantage for *in-vivo* investigations over animal models, more precisely, over rats. Rat is mostly being used as model for osteoporosis investigations. Also, the properties of Ag NPs@CS/Agar nano biocomposite against common human normal cell line i.e. HUVEC were evaluated.

2. Experimental

2.1. Materials and methods

The chemicals and solvents required in the synthesis of catalyst were purchased from Aldrich, USA. The biochemicals needed



Scheme 1 Synthetic preparation of Ag/CS-Agar bio nanocomposite.

in the bioapplications were procured from Fluka. All of them were used as such without further purifications. The animals (Wistar rats) were brought from National Institute of Nutrition, Hyderabad, India. During the catalyst characterizations, FT-IR spectra of all samples were recorded using a Bruker VERTEX 80 v spectrophotometer and done on KBr disc. Structural morphology and physicochemical properties were studied by FESEM-TESCAN MIRA3 microscope. TEM analysis was carried out with a Philips CM10 microscope at an operating voltage of 200 Kv. XRD analysis of the nanostructures was carried out using Co K α radiation ($\lambda = 1.78897 \text{ \AA}$) with operating at 40 keV, and a cathode current of 40 Ma in the scanning range of $2\theta = 5\text{--}80^\circ$.

2.2. Preparation of the Ag NPs@CS/Agar nano bio-composite

The synthesis was made based on a reported article by Veisi et al (Shahriari et al., 2021). An equal amount of chitosan

(98% decetylated NH₂) and agarose gel (0.5 g each) were dissolved in 50 mL of 1% (v/v) acetic acid solution and stirred for 3 h to obtain a chitosan/agar hydrogel composite (CS/Agar). pH of the solution was adjusted to pH 9 (NaOH, 3 wt%) and subsequently an aqueous solution of AgNO₃ (20 mg in 10 mL) was added drop-wise, at room temperature, over a period of 10 min. The mixture was then refluxed for 2 h at 100 °C. Progress of the reaction could be monitored by the change in color to gray. Finally, the reaction mixture was cooled to room temperature and the prepared Ag NPs@CS/Agar nano bio-composite were collected by centrifugation. It was washed several times with DI-water and dried at 40 °C.

2.3. Antioxidant activities of Ag NPs@CS/Agar nano bio-composite

This assay was carried out following the modified method of Lu et al (Lu et al., 2021). 0.5 mL of 0.1 mM DPPH solution

prepared in 95% ethanol was mixed with 100 μ l of Ag NPs@CS/Agar nano bio-composite. The resulting solution was kept in the dark at 38 °C for 31 min. Absorbance of the samples was then measured at 518 nm. To compare the activity of Ag NPs@CS/Agar nano bio-composite, standard BHT compound was used as a standard antioxidant.

To determine the IC₅₀ of Ag NPs@CS/Agar nano bio-composite, experiments were performed at eleven different concentrations of the desired NP solution and BHT. Each experiment was performed in three shifts and the mean values were calculated. Percentage of radicalization activity was calculated through the following equation

$$\text{Inhibition (\%)} = \frac{\text{Sample A.}}{\text{Control A.}} \times 100$$

In this regard, the blank adsorption indicates the adsorption of the control solution, which contains 0.5 mL of DPPH solution and 100 μ l of 95% ethanol instead of Ag NPs@CS/Agar nano bio-composite solution. Adsorption of the reaction indicates the adsorption of the solution containing Ag NPs@CS/Agar nano bio-composite sample.

2.4. Cytotoxicity properties of Ag NPs@CS/Agar nano bio-composite

HUVEC cells were used to evaluate the cytotoxicity of Ag NPs@CS/Agar nano bio-composite. For this purpose, each cell line was placed separately in T25 flasks with a complete culture medium [including DMEM (Dulbecco's Modified Eagle Medium), 10% complementary bovine fetal serum, and 1% penicillin–streptomycin solution] at 37 °C in the incubator and incubated in presence of 5% CO₂. After obtaining 80% cell density, the sample was exposed to 1% trypsin-EDTA solution and after 3 min of incubation at 37 °C in a cell culture incubator with 5% CO₂, the cells were removed from the bottom of the plate. The collected cells were centrifuged at 5000 rpm for 5 min and then the cell precipitate was decryped by adding trypsin culture medium. Then, the cell suspension was mixed to trypan blue dye and counted by neobar slide and cytotoxicity test was performed by MTT method. For this purpose, in each well of 96 cell culture plate, 10,000 HUVEC cells were introduced with 200 μ l from the complete cell culture medium and to achieve the cell monolayer density, the plate was re-exposed to 5% CO₂ at 37 °C. After reaching 80% cell growth, the culture medium was removed and the cell surface was first washed with PBS buffer, again, in all wells, a complete two-concentration culture medium of 100 μ l was introduced. 100 μ l of a solution of Ag NPs@CS/Agar nano bio-composite dissolved in PBS (mg/mL²) was then introduced into well No. 1. After mixing the nanoparticles in the culture medium, 100 μ l of it was removed and added to the second well. In the next step, 100 μ l of the second well was removed after stirring the medium and added to well 3. This operation was performed up to well 11 and thus the amount of nanoparticles in each well was halved, respectively. Well No. 12 contained only one cell and complete culture medium of one concentration and remained as a control. The plate was again exposed to 5% CO₂ at 37 °C for 24 h and then the cytotoxicity was determined using tetrazolium dye. 10 μ l of tetrazolium dye (5 mg/ml) was added to all wells, including the control, and the plate was exposed to 5% CO₂ at 37 °C for 2 h. The dye was

then removed from the wells and 100 μ l of DMSO (Dimethyl sulfoxide) was added to the wells, the plate was wrapped in aluminum foil and shaken thoroughly in a shaker for 20 min. Finally, cell survival was recorded in ELISA reader at 540 nm

$$\text{Cell viability (\%)} = \frac{\text{Sample A.}}{\text{Control A.}} \times 100$$

Then, based on the absorption rate of each well and its comparison with the control, the inhibitory concentration of 50% (IC₅₀) was obtained.

2.5. Anti-osteoporosis properties of Ag NPs@CS/Agar nano bio-composite over animals

24 young male rats of Wistar strain weighing 150–250 g were kept protected in a temperature controlled room (24 \pm 1 °C) with 12:12 h L:D illumination cycle. All animals were allowed free access to distilled water and fed on a commercial diet.

2.5.1. Induction of osteoporosis and experimental design

Animals were divided into following four groups of 6 rats each. Gr. I were negative control animals treated with saline. Osteoporosis was induced in male rats by injecting methyl prednisolone sodium succinate, a glucocorticoid (GC) in a dose of 10 mg/kg thrice a week for four weeks by subcutaneous route. Gr. 2 animals received GC alone. Gr. 3 were GC treated animals which received risedronate sodium (20 μ g/kg, sc) as a standard, five times a week for the next 30 days. Gr. 4 were GC treated animals which received the Ag NPs@CS/Agar nano bio-composite (5 μ g/kg/day, po, for 30 days) daily by oral route for the next 30 days.

2.5.2. Biochemical analysis

After 60 days, the rats were anaesthetized with enflurane and blood was withdrawn from the retro orbital plexus and collected into dry test tubes. It was centrifuged at 3000 rpm for 10 min for the separation of serum. The separated serum was used for biochemical analysis. Bone mineral content markers-Calcium was estimated by oCPC method in which it complexes with o-cresolphthalein complexone. Phosphorous was estimated by molybdate UV method.

2.5.3. Bone resorption markers

Creatinine was estimated by Jaffe's kinetic method. Serum specific alkaline phosphatase was estimated by PNPP kinetic method in the serum using standard kits with a semi auto analyzer (ErbaChem 5 Plus V2). Hydroxyproline was estimated in urine using modified Switzer and Summer. The levels of serum chemistries of bone mineral content and bone resorption markers were measured using a semi-automatic analyzer (ERBA Chem-5 Plus V2, Transasia Bio-Medicals Ltd, Mumbai).

2.5.4. Physical and biomechanical parameters

The animals were sacrificed on 60 day after blood withdrawal. Femur and tibia were isolated, defleshed and immediately weighed. The length of bones was determined using dial calipers. Assessment of their biomechanical strength was done

by using Universal testing machine (UTE 40 HGFL; Fuel Instruments and Engineers Ltd).

2.5.5. Three point bending test of femur and tibia

The bones were placed horizontally on two supporting bars separated at a distance of 15 mm and was loaded by a rounded press. Bones were subjected to test with loading at a speed of 1 mm/min each mm corresponding to 40 Newton (N) perpendicular to the bone longitudinal axis. Variables estimated were yield load which is the force causing the first detectable bone damage and ultimate load which is the force at which fracture occurs.

2.5.6. Compression test of femur and tibia

The bones were placed on the flat metallic stage and compressed until it fractured. The reading was recorded in Newton (N).

2.6. Statistical analysis

After collecting data, Minitab statistical software was used for statistical analysis. Evaluation of antioxidant results in a completely randomized design and comparison of means was Duncan post-hoc test with a maximum error of 5%. To measure the percentage of cell survival in factorial experiments with the original design of completely randomized blocks and compare the means, Duncan post-hoc test with a maximum error of 5% was used. The 50% cytotoxicity (IC50) and 50% free radical scavenging (IC50) was estimated with ED50 plus software (INER, V: 1.0). Measurements were reported as mean \pm standard deviation.

3. Results and discussion

3.1. Structural characterization of synthesized Ag NPs@CS/Agar nano bio-composite

FT-IR spectra were recorded to identify the changes in the physiological features of CS/Agar bio-composite upon green immobilized Ag NPs. Fig. 1 displays a comparative FT-IR spectra of CS, agar, CS/Agar and Ag NPs@CS/Agar nano bio-composite. The characteristic absorption bands of chitosan are represented in Fig. 1a as, 1028 cm^{-1} (C–N stretching), 1382 cm^{-1} (C–O stretching of $\text{CH}_2\text{-OH}$ linkage), 1591 cm^{-1} (N–H bending), 1648 cm^{-1} (C = O stretching of amide linkage) and 3400–3500 cm^{-1} (O–H and N–H stretching) (Veisi et al., 2020). In the FT-IR spectra of agar (Fig. 1b) the broad peak appeared at 3425 cm^{-1} corresponds to the overlapped stretching vibrations of OH groups. The alcoholic C–O stretching and O–H bending peaks are observed at 1075 cm^{-1} and 1659 cm^{-1} respectively (Shahriari et al., 2021). Agar is a polysaccharide composite made of glucuronic and pyruvic acid which contains carbonyl function, vibration of which may also be merged into the O–H bending region. Fig. 1c, representing the FT-IR spectrum of CS/Agar composite, which the most significant adsorption bands of chitosan and agar substrates are present with slight shift. And finally in the spectrum of Ag NPs@CS/Agar nano bio-composite (Fig. 1d), because of interactions of the functional groups of CS/Agar with Ag nanoparticles, the corresponding IR

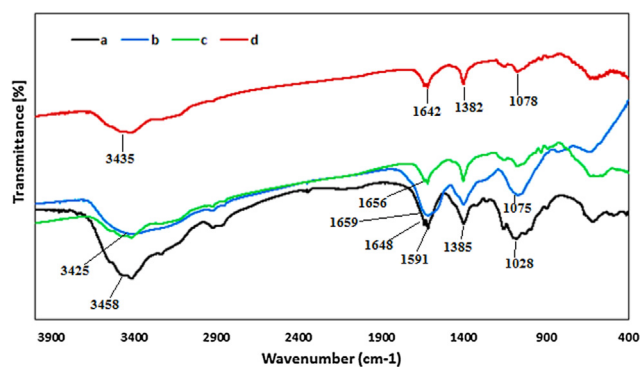


Fig. 1 FT-IR spectra of (a) CS, (b) Agar, (c) CS/Agar and (d) Ag NPs@CS/Agar nano bio-composite.

absorption bands are observed to be shifted to higher or lower regions respectively.

Structural morphology, shape and size and of the as-synthesized Ag NPs@CS/Agar nano bio-composite were investigated by FE-SEM and TEM analysis. Fig. 2 displays the FE-SEM image with pseudo-spherical shaped particles. A homogeneous layer of the hydrogel polymers over the surface can be seen on close observation. This makes the particles fluffy. Due to high surface energy, the particles have high tendency to agglomerate forming lump like appearances. Some more detailed structural features are obtained from TEM images (Fig. 3). They are spherical shapes and mono dispersed with an average particle diameter of 10–15 nm. Moreover, Fig. 3 determines the particle size distribution histogram for Ag NPs whose average size are approximately 12.25 nm respectively.

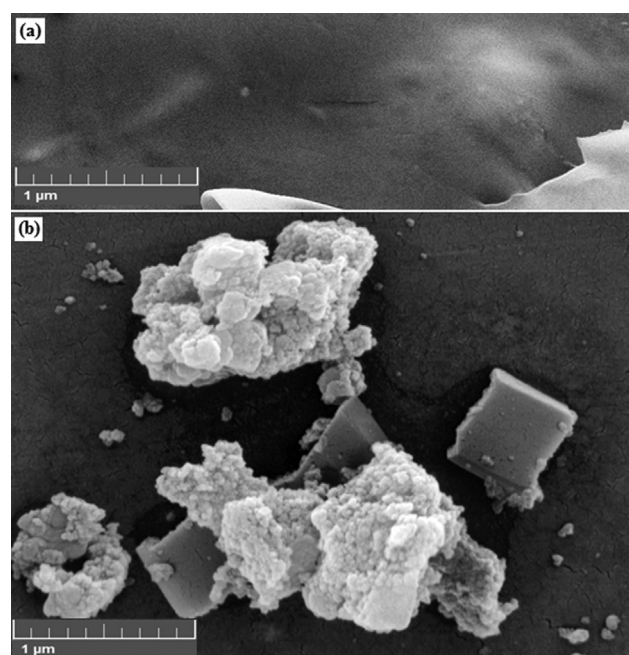


Fig. 2 FE-SEM images of the (a) CS/Agar hydrogel and (b) Ag NPs@CS/Agar nano bio-composite.

EDX analysis was performed to confirm the presence of silver species on the composite. EDX spectrum of Ag NPs@CS/Agar nano bio-composite in Fig. 4 clearly confirms the presence of Ag metal on CS/Agar composite. However, some other peaks of C, N and O as constitutional element are also observed. These non-metals can be assigned to the CS/Agar composite.

To verify the conversion of Ag(I) to Ag(0) over CS/Agar surface and also determining the crystallinity and phase structure, XRD analysis of the Ag NPs@CS/Agar nano-composite was performed and the outcome is shown in Fig. 5. Three characteristic peaks at 38.2° , 44.3° , 64.6° and 77.3° , which corresponded to (111), (200), (220) and (311) crystallographic planes of the Ag NPs, can clearly be seen in the spectrum. These sharp peaks confirm that Ag NPs have been successfully stabilized on the surface of CS/Agar composite. The initial phase in the 2θ region up to 20° was attributed to CS/Agar composite and being non-crystalline.

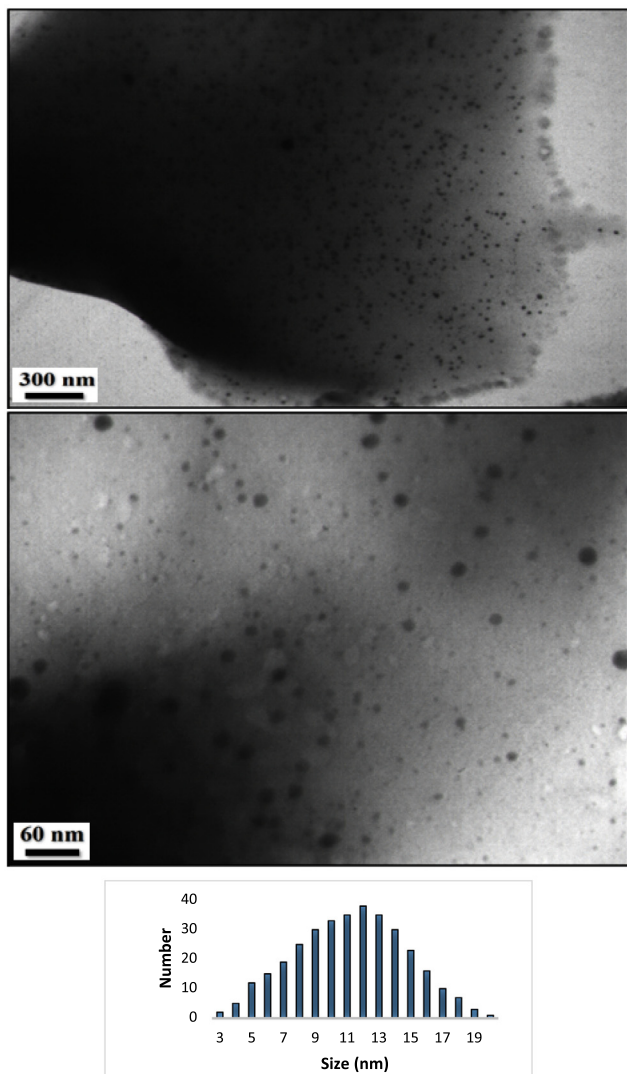


Fig. 3 TEM images of the Ag NPs@CS/Agar nano bio-composite and particle size distribution histogram for Ag NPs.

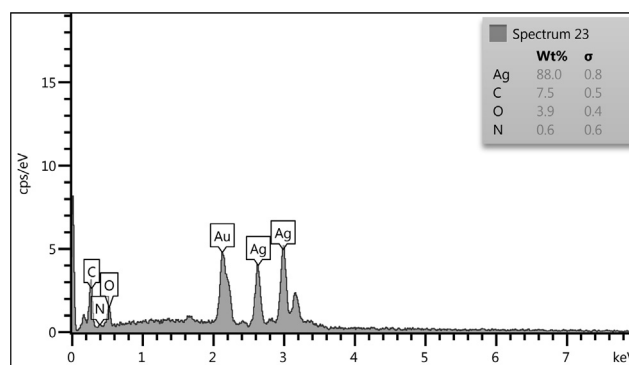


Fig. 4 EDX spectrum of the Ag NPs@CS/Agar nano bio-composite.

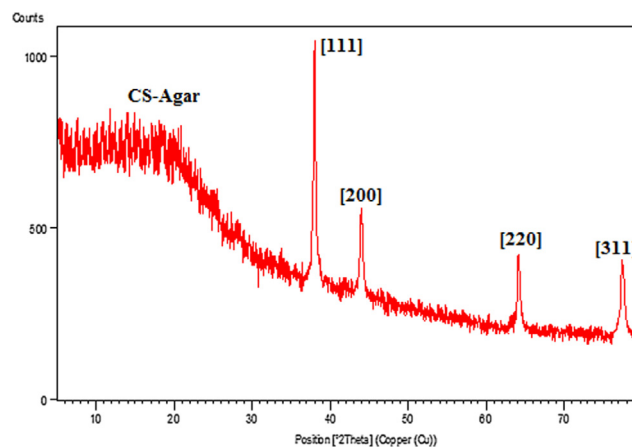


Fig. 5 XRD pattern of the Ag NPs@CS/Agar nano bio-composite.

3.2. Antioxidant effects analysis of Ag NPs@CS/Agar nano bio-composite

Oxidative stress is caused by an imbalance between the production of free radicals and metabolic reactions, which leads to damage to lipids, proteins and nucleic acids. These damages may be due to low levels of antioxidants or an excessive increase in the production of free radicals in the body (Namvar et al., 2014; Sankar et al., 2014; Katata-Seru et al., 2018). In humans, oxidative stress is associated with chronic diseases such as diabetes and cancer. Therefore, the production of synthetic and natural antioxidants is necessary to prevent oxidative stress and its destructive effects. Antioxidants effectively and in various ways reduce the harmful effects of free radicals in the biological and food systems and cause detoxification (Sangami and Manu, 2017). In this regard, green nanoparticles can be used (using plant substrates to prepare nanomaterials that are environmentally friendly and do not contain any harmful chemicals) that show antioxidant properties. At present, the use of non-toxic substances in synthesizing nanoparticles to prevent biological hazards, especially in medical and pharmaceutical applications is considered (Namvar et al., 2014; Sankar et al., 2014; Katata-Seru et al., 2018; Sangami and Manu, 2017; Beheshtkhoo et al., 2018; Radini et al., 2018). Many researchers have focused on bioactive sub-

stances derived from plants or other sources such as bacteria, fungi and yeast for synthesizing nanoparticles. The green synthesis method is thought to increase the biocompatibility and performance of metal nanoparticles for biological applications due to removing harmful chemicals (Namvar et al., 2014; Sankar et al., 2014; Katata-Seru et al., 2018). During the bio-production stages of nanoparticles, their extracellular production using plants or their extracts is more beneficial and their production can be adjusted in a controlled way based on size, distribution and shape for different purposes. In the recent study, the scavenging capacity of Ag NPs@CS/Agar nano bio-composite and BHT at different concentrations expressed as percentage inhibition has been indicated in Table 1 and Fig. 6. In the antioxidant test, the IC₅₀ of them against DPPH free radicals were observed 120 and 104 µg/mL, respectively (Table 1).

3.3. Cytotoxicity study of Ag NPs@CS/Agar nano-composite over HUVEC cell lines

Ag NPs are used in many commercial products, including soap, food, plastics, catheters, textiles, and bandages. Many factors (shape, size, surface chemistry, morphology, density, charge, and purity) affect the biological activity of them. Another important feature of Ag NP is their role in treating cancer. They are used as a promising tool as anti-cancer agent in diagnosis and evaluation. They have many benefits with strong effects against different cancer cell lines. Their better penetration and ability to detect cancer cells in the body make them a more effective tool in treating low-risk cancers compared to standard treatments. Ag NPs can also be conjugated to various molecules, including DNA and RNA, to target different cells and antibodies or polymers (Beyene et al., 2017; Chen and Schluessener, 2008; Alexander, 2009; Jo et al., 2015; Rai et al., 2014). They induce changes in cell morphology, decrease cell metabolic activity, increase oxidative stress leading to mitochondrial damage, and ultimately damage DNA by producing reactive oxygen species (ROS). Adsorption of them occurs through endocytosis (Riehemann et al., 2009; Huang et al., 2017; Conde et al., 2012; Bhattacharyya et al., 2011). Ag NPs, like other biomaterials, can cause toxic effects in living organisms. The toxicity induced by is due to oxidative stress, which accumulates in the cytoplasm and cell nucleus, leading to the production of free radicals (Huang et al., 2017; Conde et al., 2012). In this investigation, the cytotoxicity of Ag NPs/CS-Agar bio-composite were assessed over normal HUVEC cell lines in different concentrations following MTT assay for 48 h and compared the results with AgNO₃ treatment. Fig. 7 displays the corresponding results where % cell viability of the nanocomposite becomes much lower as compared to AgNO₃, with increasing concentration.

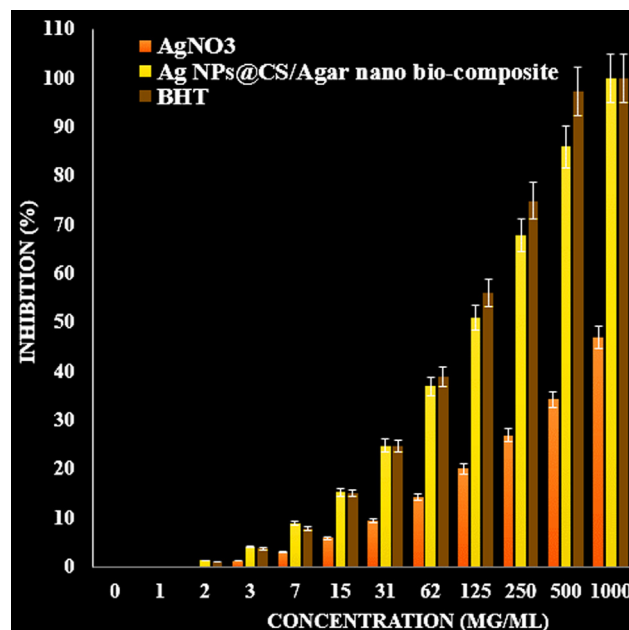


Fig. 6 The antioxidant properties of AgNO₃, Ag NPs@CS/Agar nano bio-composite, and BHT against DPPH.

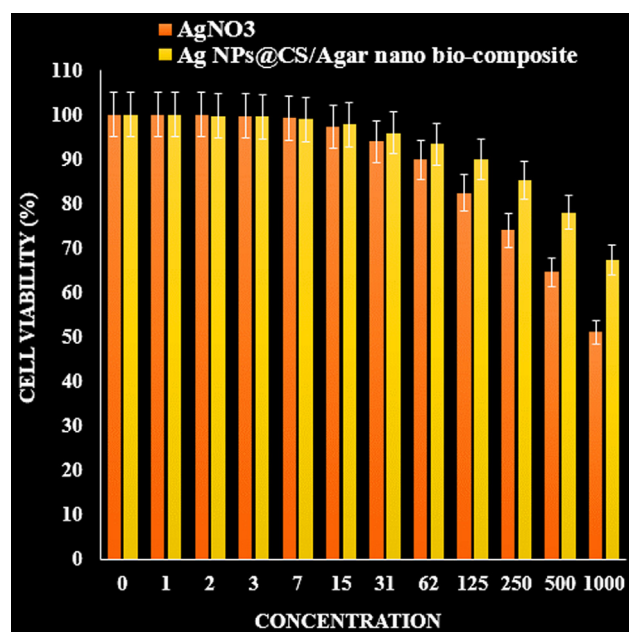


Fig. 7 The cytotoxicity effects of AgNO₃ and Ag NPs@CS/Agar nano bio-composite against normal (HUVEC) cell line.

Table 1 The IC₅₀ of AgNO₃, Ag NPs@CS/Agar nano bio-composite, and BHT in antioxidant test.

	AgNO ₃ (µg/mL)	Ag NPs@CS/Agar nano bio-composite (µg/mL)	BHT (µg/mL)
IC ₅₀ against DPPH	–	120 ± 0	104 ± 0

3.4. Anti-osteoporosis properties of Ag NPs@CS/Agar nano bio-composite

Anti-osteoporosis effect exhibited by different nanoparticles is believed to be due to their antioxidant effects. As the disease progression is very closely linked to inflammation and oxidative stress, a compound with anti-inflammatory or antioxidant properties can be an anti-osteoporosis agent (Namvar et al., 2014; Sankar et al., 2014). In recent times, nanoparticles synthesized by biological methods play a vital role in treating many diseases, including osteoporosis (Katata-Seru et al., 2018; Sangami and Manu, 2017; Beheshtkhoo et al., 2018; Radini et al., 2018). They are used not only as traditional medicine, but also have been able to adopt an industrial line of natural products for treating various diseases.

Recently, methyl prednisolone sodium succinate, a glucocorticoid has been used for inducing osteoporosis in rats. Glucocorticoids modify osteoblastic cell differentiation, number, and function. They stimulate the osteoclastogenesis and increase the expression of receptor activator of Nuclear factor-kappa B ligand and colony-stimulating factor-1, and decrease the expression of osteoprotegerin. However, the most significant effect of glucocorticoids in bone is an inhibition of bone formation. This inhibition is caused by a decrease in the number of osteoblasts secondary to a shift in the differentiation of mesenchymal cells away from the osteoblastic lineage, and an increase in the death of mature osteoblasts. Glucocorticoids decrease the function of the remaining osteoblasts directly and indirectly through the inhibition of insulin-like growth factor I expression. The stimulation of bone resorption

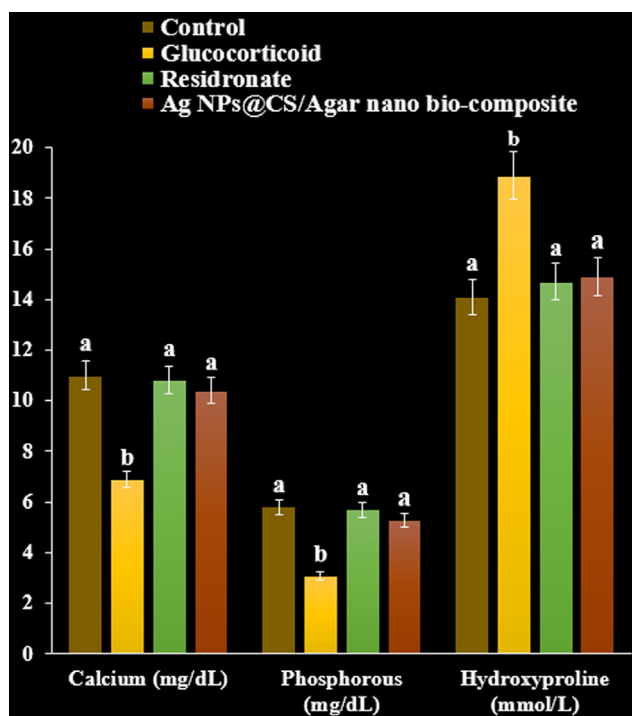


Fig 8 The effect of Ag NPs@CS/Agar nano bio-composite on calcium, phosphorous, and hydroxyproline concentrations in osteoporosis induced by Glucocorticoid in rats.

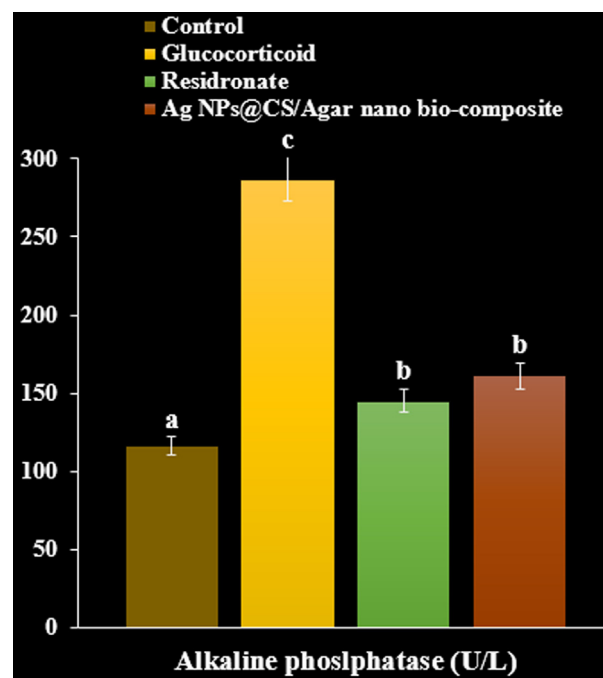


Fig 9 The effect of Ag NPs@CS/Agar nano bio-composite on alkaline phosphatase concentration in osteoporosis induced by Glucocorticoid in rats.

is likely responsible for the initial bone loss after glucocorticoid exposure. Eventually, the inhibition of bone formation causes a decrease in bone remodeling and a continued increased risk of fractures (Raimundo et al., 2017). In this connection we have employed the Ag NPs@CS/Agar nano bio-composite in determining the anti-osteoporotic activities.

3.4.1. Effect of Ag NPs@CS/Agar nano bio-composite on biochemical parameters

As can be seen at the Figs. 8-10, Ag NPs@CS/Agar nano bio-composite caused a significant rise in serum calcium and phosphorus compared with GC treated group ($P < 0.05$). GC produced an elevation in levels of alkaline phosphatase and creatinine. Treatment with risedronate and Ag NPs@CS/Agar nano bio-composite evoked a reduction in the levels of alkaline phosphatase and creatinine compared with GC treated group ($P < 0.05$). GC treated group exhibited a significant rise in urinary hydroxyproline levels compared to negative control ($P < 0.05$). Treatment with risedronate and Ag NPs@CS/Agar nano bio-composite produced a decline in the levels of urinary hydroxyproline compared to GC treated group ($P < 0.05$).

3.4.2. Effect of Ag NPs@CS/Agar nano bio-composite on physical and biomechanical parameters

A significant decrease in femur and tibia weight and length was observed in methyl prednisolone treated rats compared to negative control group ($P < 0.05$). Bone weight and length found significantly increased on treatment with risedronate, and Ag NPs@CS/Agar nano bio-composite respectively compared with GC treated group ($P < 0.05$, Fig. 11, Fig. 12).

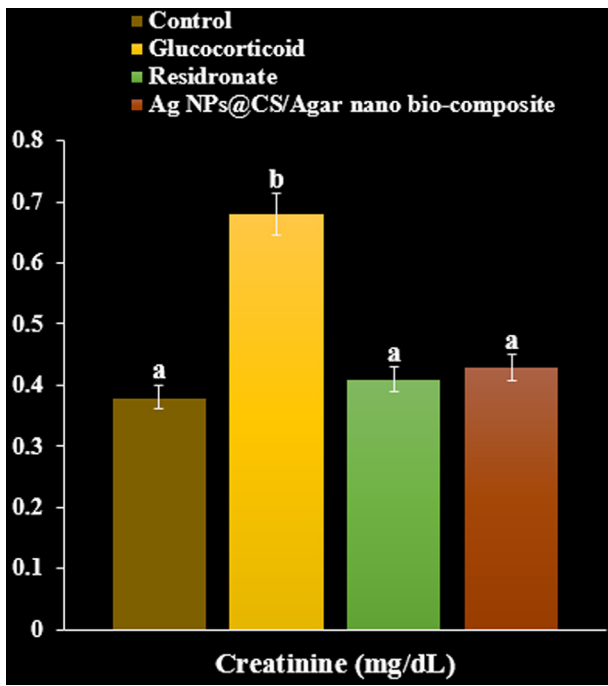


Fig 10 The effect of Ag NPs@CS/Agar nano bio-composite on creatinine concentration in osteoporosis induced by Glucocorticoid in rats.

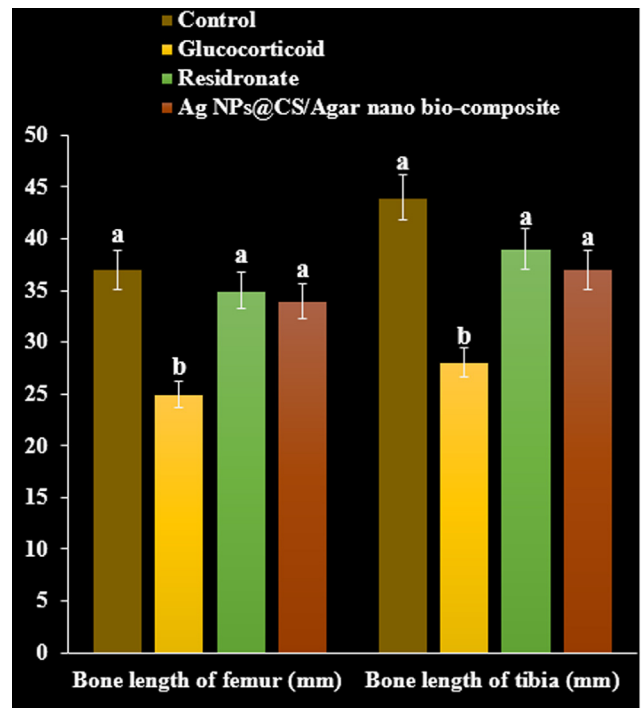


Fig 12 The effect of Ag NPs@CS/Agar nano bio-composite on bone length of femur and tibia in osteoporosis induced by Glucocorticoid in rats.

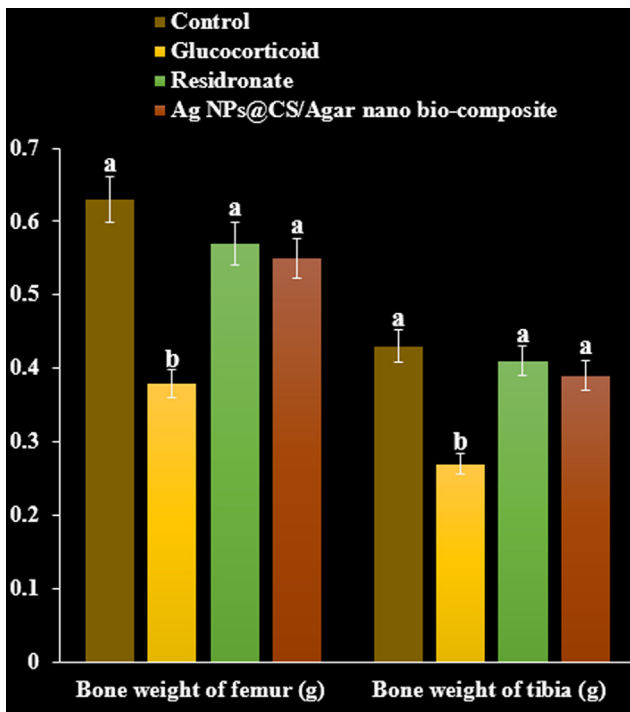


Fig 11 The effect of Ag NPs@CS/Agar nano bio-composite on bone weight of femur and tibia in osteoporosis induced by Glucocorticoid in rats.

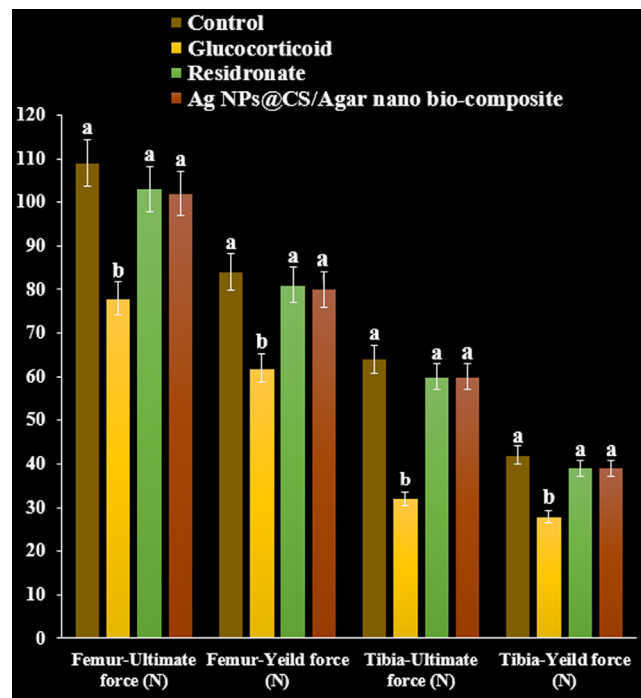


Fig 13 The effect of Ag NPs@CS/Agar nano bio-composite on yield and ultimate forces (Femur and tibia) using three points test in osteoporosis induced by Glucocorticoid in rats.

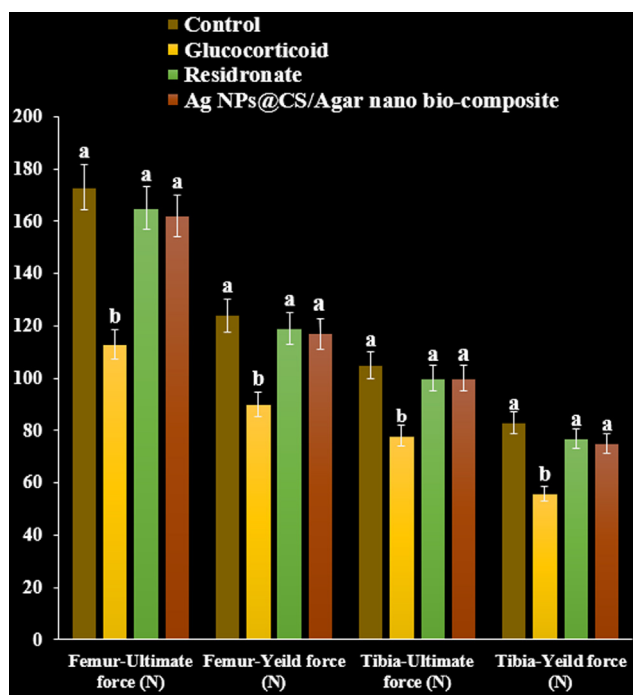


Fig 14 The effect of Ag NPs@CS/Agar nano bio-composite on yield and ultimate forces (Femur and tibia) using compression test in osteoporosis induced by Glucocorticoid in rats.

3.4.3. Three point bending test of femur and tibia

The ultimate load tolerated by femur and tibia in rats treated with GC declined to in the three point bending test and compression test compared with the control ($P < 0.05$). Load tolerated by risedronate treated rats increased in both the three point and compression test. Maximum load required to fracture the femur and tibia increased significantly following treatment with Ag NPs@CS/Agar nano bio-composite compared with GC treated group ($P < 0.05$, Figs. 13 and 14).

4. Conclusion

In conclusion, we demonstrate the design and synthesis of a novel Ag NP adorned chitosan/agar bio-composite matrix following a sustainable pathway without using any toxic reducing agents. To elucidate the chemical structure of the as-synthesized nano bio-composite, FT-IR, FE-SEM, EDX, TEM and XRD analyses were performed and justified the physicochemical properties. Towards its bioapplication, we evaluated the anti oxidant activity, cytotoxicity and anti-osteoporotic effects of the Ag NPs@CS/Agar nano bio-composite. Cell viability of the normal HUVEC cell line was found to be reduced dose-dependently in presence of the catalyst. The absorbances were measured at 570 nm, which represented viability of normal cell line even up to 1000 $\mu\text{g/mL}$ for Ag NPs/CS-Starch bio-composite. The Ag NPs@CS/Agar nano bio-composite showed excellent antioxidant activities in DPPH radical scavenging assay. The IC₅₀ of Ag NPs@CS/Agar nano bio-composite and BHT in the study were 120 and 104 $\mu\text{g/mL}$, respectively. Again, administration of Ag NPs@CS/Agar nano bio-composite on the GC induced Wistar

rats showed an increase in the serum levels of bone mineral content markers and a decrease in serum and urinary levels of bone resorption markers. An inclination in the strength of femur and tibia was seen particularly with Ag NPs@CS/Agar nano bio-composite. Maintenance of calcium homeostasis, formation of collagen and scavenging of free radicals can plausibly be the mode of action of Ag NPs@CS/Agar nano bio-composite thereby combating osteoporosis induced by glucocorticoids.

Declaration of Competing Interest

The authors declare that they have no known competing financial interests or personal relationships that could have appeared to influence the work reported in this paper.

Acknowledgments:

The authors extend their appreciation to Taif University for supporting this work. Researchers Supporting Project under project number (TURSP-2020/116), Taif University, Taif, Saudi Arabia. Also, the authors would like to thank the Deanship of Scientific Research at King Khalid University, Abha, KSA for funding this work under Grant number (R.G. P.2/47/42).

I have to add that this submission is original and all co-authors are aware of the submission and agree to its publication in the *Arab J Chem*. This work is novel/original and is not under consideration for publication elsewhere.

References

- Alexander, J.W., 2009. History of the medical use of silver. *Surg. Infect.* 10, 289–292.
- Andersen, T., Christensen, F.B., Langdahl, B.L., Ernst, C., Frøensgaard, S., Østergaard, J., Andersen, J.L., Rasmussen, S., Niedermann, B., Høy, K., Helmig, P., Holm, R., Egund, N., Bünger, C., 2013. Degenerative spondylolisthesis is associated with low spinal bone density: a comparative study between spinal stenosis and degenerative spondylolisthesis. *Biomed Res Int* 2013, 1–8.
- Aswathy Aromal, S., Philip, D., 2012. Green synthesis of gold nanoparticles using *Trigonella foenum-graecum* and its size-dependent catalytic activity. *Spectrochim. Acta Part A* 97, 1–5.
- Barry, M., Pearce, H., Cross, L., Tatullo, M., Gaharwar, A.K., 2016. *Advances in Nanotechnology for the Treatment of Osteoporosis*. *Curr Osteoporos Rep.* 14, 87–94.
- Beheshtkhoo, N., Kouhbanani, M.A.J., Savardashtaki, A., et al, 2018. Green synthesis of iron oxide nanoparticles by aqueous leaf extract of *Daphne mezereum* as a novel dye removing material. *Appl Phys A* 124, 363–369.
- Beyene, H.D., Werkneh, A.A., Bezabh, H.K., Ambaye, T.G., 2017. Synthesis paradigm and applications of silver nanoparticles (Ag NPs), a review. *Sustain. Mater. Technol.* 13, 18–23.
- Bhattacharyya, S., Kudgus, R.A., Bhattacharya, R., Mukherjee, P., 2011. Inorganic nanoparticles in cancer therapy. *Pharm. Res.* 28, 237–259.
- Bultink, I.E.M., Baden, M., Lems, W.F., 2013. Glucocorticoid-induced osteoporosis: an update on current pharmacotherapy and future directions. *Expert Opin. Pharmacother.* 14 (2), 185–197.
- Chen, X., Schluesener, H.J., 2008. Nanosilver: A nanoparticle in medical application. *Toxicol. Lett.* 176, 1–12.
- Conde, J., Doria, G., Baptista, P., 2012. Noble metal nanoparticles applications in cancer. *J. Drug Deliv.* 2012, 751075.

- Ding, W., Liang, Z., El-Kott, A.F., El-Kenawy, A.E., 2021. Investigation of anti-human ovarian cancer effects of decorated Au nanoparticles on Thymbraspicata extract modified Fe₃O₄ nanoparticles. *Arabian J. Chem.* 14, (7) 103205.
- Ding, Z., Shi, H., Yang, W., 2019. Osteoprotective Effect of Cimracemate in Glucocorticoid-Induced Osteoporosis by Osteoprotegerin/Receptor Activator of Nuclear Factor κ B/Receptor Activator of Nuclear Factor Kappa-B Ligand Signaling. *Pharmacology* 103 (3-4), 163–172.
- Dushyanthen, S., Cossigny, D.A., Quan, G.M., 2013. The osteoblastic and osteoclastic interactions in spinal metastases secondary to prostate cancer. *Cancer Growth Metastasis* 6, 61–80.
- (a) M. Entezari, M. Safari, M. Hekmati, S. Hekmat, A. Azin, *Med. Chem. Res.* 23 (2014) 487-495; (b) M Hajighorbani, M Hekmati, *RSC advances*, 2016,6, 88916-88924; (c) J. Azizian, M. Hekmati, O. G. Dadras, *Orient J Chem* 30 (2014) 667-673; (d) M.H. Salehi, M. Yousefi, M. Hekmati, E. Balali, *Polyhedron* 165 (2019) 132-137; (e) Z. Karimi Ghezeli, M. Hekmati, H. Veisi, *Applied Organometallic Chemistry* 33 (2019) e4833; (f) R. Ghorbani-Vaghei, S. Hemmati, M. Hekmati, *Journal of Chemical Sciences* 128 (2016) 1157-1162; (g) Wei Zhang, Hojat Veisi, Reyhaneh Sharifi, Delafarin Salamat, Bikash Karmakar, Malak Hekmati, Saba Hemmati, Mohammad Mahdi Zangeneh, Zhiyong Zhang, Qiang Su, *Int J Biological Mac.* 160 (2020) 1252-1262; (h) H. Veisi, Y. Metghalchi, M. Hekmati, S. Samadzadeh, *Appl. Organomet. Chem.* 31 (2017) e3676.
- Fratoddi, I., Carloni, A., Catone, D., O’Keeffe, P., Paladini, A., Toschi, F., Turchini, S., Sciubba, F., Testa, G., Battocchio, C., Carlini, L., Zaccaria, R.P., Magnano, E., Pis, I., Avaldi, L., 2018. Gold nanoparticles functionalized by rhodamine B isothiocyanate to tune plasmonic effects. *J. Colloid Interf. Sci.* 513, 10–19.
- Gomes, H.I.O., Martins, C.S.M., Prior, J.A.V., 2021. Nanoparticles as Carriers of Anticancer Drugs for Efficient Target Treatment of Cancer Cells. *Nanomaterials* 11, 964.
- Gudbjornsson, B., Juliusson, U.I., Gudjonsson, F.V., 2002. Prevalence of long term steroid treatment and the frequency of decision making to prevent steroid induced osteoporosis in daily clinical practice. *Ann. Rheum. Dis.* 61, 32–36.
- Y. Huang, Y. Kang, A. El-kott, A. E. Ahmed, A. Khames, M. A. Zein, Decorated Cu NPs on Lignin coated magnetic nanoparticles: Its performance in the reduction of nitroarenes and investigation of its anticancer activity in A549 lung cancer cells, *Arab. J. Chem.* 14, 2021,103299.
- Huang, Y., Fan, C.Q., Dong, H., Wang, S.M., Yang, X.C., Yang, S. M., 2017. Current applications and future prospects of nanomaterials in tumor therapy. *Int. J. Nanomed.* 12, 1815–1825.
- Huy, T.Q., Huyen, P.T.M., Le, A.T., Tonezzer, M., 2020. Anticancer Agents *Med Chem* 20 (11), 1276–1287.
- I. Ilias, E. Zoumakis, H. Ghayee, An overview of glucocorticoid induced osteoporosis; in L. J. De Groot, G. Chrousos K. Dungan, et al., (eds): *Endotext* [Internet]. South Dartmouth, MDText. com, Inc., 2000.
- Jia, J., Yao, W., Guan, M., Dai, W., Dai, W., Shahnazari, M., Kar, R., Bonewald, L., Jiang, J.X., Lane, N.E., 2011. Glucocorticoid dose determines osteocyte cell fate. *FASEB J* 25, 3366–3376.
- Jo, D.H., Kim, J.H., Lee, T.G., Kim, J.H., 2015. Size, surface charge, and shape determine therapeutic effects of nanoparticles on brain and retinal diseases. *Nanomed Nanotechnol. Biol. Med.* 11, 1603–1611.
- Kanis, J.A., McCloskey, E.V., Johansson, H., Oden, A., Melton, L.J., Khaltaev, N.A., 2008. Reference Standard for the Description of Osteoporosis. *Bone* 42, 467–475.
- Katata-Seru, L., Moremedi, T., Aremu, O.S., et al, 2018. Green synthesis of iron nanoparticles using *Moringaoleifera* extracts and their applications: Removal of nitrate from water and antibacterial activity against *Escherichia coli*. *J Mol Liq* 256, 296–304.
- Khan, A.A., Morrison, A., Hanley, D.A., Felsenberg, D., McCauley, L.K., O’Ryan, F., Reid, I.R., Ruggiero, S.L., Taguchi, A., Tetradis, S., Watts, N.B., Brandi, M.L., Peters, E., Guise, T., Eastell, R., Cheung, A.M., Morin, S.N., Masri, B., Cooper, C., Morgan, S.L., Obermayer-Pietsch, B., Langdahl, B.L., Al Dabagh, R., Davison, K.S., Kendler, D.L., Sándor, G.K., Josse, R.G., Bhandari, M., El Rabbany, M., Pierroz, D.D., Sulimani, R., Saunders, D.P., Brown, J.P., Compston, J., 2015. Diagnosis and management of osteonecrosis of the jaw: a systematic review and international consensus. *J. Bone Miner. Res.* 30 (1), 3–23.
- Lin, S., Huang, J., Zheng, L., Liu, Y., Liu, G., Li, N., Wang, K., Zou, L., Wu, T., Qin, L., Cui, L., Li, G., 2014. Glucocorticoid-Induced Osteoporosis in Growing Rats. *Calcif. Tissue Int.* 95 (4), 362–373.
- Loo, Y.Y., Rukayadi, Y., Nor-Khaizura, M., Kuan, C.H., Chieng, B. W., Nishibuchi, M., Radu, S., 2018. *In Vitro* Antimicrobial Activity of Green Synthesized Silver Nanoparticles Against Selected Gram-negative Foodborne Pathogens. *Front. Microbiol.* 9, 1555.
- Lu, Y., Wan, X., Li, L., Sun, P., Liu, G., 2021. Synthesis of a reusable composite of graphene and silver nanoparticles for catalytic reduction of 4- nitrophenol and performance as anti-colorectal carcinoma. *J Mater Res Technol.* 12, 1832–1843.
- Mora-Raimundo, P., Lozano, D., Manzano, M., Vallet-Regí, M., 2019. Nanoparticles to Knockdown Osteoporosis-Related Gene and Promote Osteogenic Marker Expression for Osteoporosis Treatment. *ACS Nano* 13 (5), 5451–5464.
- Moshiri, A., Sharifi, A.M., Oryan, A., 2017. Current Knowledge, Drug- Based Therapeutic Options and Future Directions in Managing Osteoporosis. *Clin. Rev. Bone Miner. Metab.* 15 (1), 1–23.
- Namvar, F., Rahman, H.S., Mohamad, R., et al, 2014. Cytotoxic effect of magnetic iron oxide nanoparticles synthesized via seaweed aqueous extract. *Int J Nanomedicine* 19, 2479–2488.
- Nluan, W., Yuxiao, L., Helena, N.H., et al, 2015. Systemic drug delivery systems for bone tissue regeneration-a mini review. *Curr Pharm. Design* 21, 1575–1583.
- Oueslati, M.H., Tahar, L.B., Harrath, A.H., 2020. Catalytic, antioxidant and anticancer activities of gold nanoparticles synthesized by kaempferol glucoside from *Lotus leguminosae*. *Arab. J. Chem.* 13, 3112–3122.
- Pizzino, G., Irrera, N., Galfò, F., Oteri, G., Atteritano, M., Pallio, G., Mannino, F., D’Amore, A., Pellegrino, E., Aliquo, F., Anastasi, G. P., Cutroneo, G., Squadrito, F., Altavilla, D., Bitto, A., 2017. Adenosine Receptor Stimulation Improves Glucocorticoid-Induced Osteoporosis in a Rat Model. *Front. Pharmacol.* 8. <https://doi.org/10.3389/fphar.2017.00558>.
- Radini, I.A., Hasan, N., Malik, M.A., et al, 2018. Biosynthesis of iron nanoparticles using *Trigonellafoenum-graecum* seed extract for photocatalytic methyl orange dye degradation and antibacterial applications. *J Photochem Photobiol B* 183, 154–163.
- Rai, M., Kon, K., Ingle, A., Duran, N., Galdiero, S., Galdiero, M., 2014. Broad-spectrum bioactivities of silver nanoparticles: The emerging trends and future prospects. *Appl. Microbiol. Biotechnol.* 98, 1951–1961.
- Raimundo, P.M., Manzano, M., Vallet-Regi, M., 2017. Nanoparticles for the treatment of osteoporosis. *AIMS Bioengineering* 4 (2), 259–274.
- Riehemann, K., Schneider, S.W., Luger, T.A., Godin, B., Ferrari, M., Fuchs, H., 2009. Nanomedicine– challenge and perspectives. *Angew. Chem.* 48, 872–897.
- Rossi, A., Donati, S., Fontana, L., Porcaro, F., Battocchio, C., Proietti, E., Venditti, I., Bracci, L., Fratoddi, I., 2016. Negatively charged gold nanoparticles as dexamethasone carrier: stability and cytotoxic activity. *RCS Adv.* 6, 99016–99022.
- Rutkowski, J.L., 2011. Combined use of glucocorticoids and bisphosphonates may increase severity of bisphosphonate-related osteonecrosis of the jaw. *J. Oral Implantol.* 37, 505.
- Salamanna, F., Gambardella, A., Contartese, D., Visani, A., Fini, M., 2021. Nano-Based Biomaterials as Drug Delivery Systems Against Osteoporosis: A Systematic Review of Preclinical and Clinical Evidence. *Nanomaterials* 11, 530.

- Sangami, S., Manu, M., 2017. Synthesis of Green Iron Nanoparticles using Laterite and their application as a Fenton-like catalyst for the degradation of herbicide Ametryn in water. *Environ. Technol. Innov.* 8, 150–163.
- Sankar, R., Maheswari, R., Karthik, S., et al, 2014. Anticancer activity of *Ficus religiosa* engineered copper oxide nanoparticles. *Mater Sci Eng C* 44, 234–239.
- Shahriari, M., Sedigh, M.A., Mahdavian, Y., Mahdigholizad, S., Pirhayati, M., Karmakar, B., Veisi, H., 2021. In situ supported Pd NPs on biodegradable chitosan/agarose modified magnetic nanoparticles as an effective catalyst for the ultrasound assisted oxidation of alcohols and activities against human breast cancer. *Int. J. Biol. Macromol.* 172, 55–65.
- Z. Shi, Y. Mahdavian, Y. Mahdavian, S. Mahdigholizad et al, Cu immobilized on chitosan-modified iron oxide magnetic nanoparticles: Preparation, characterization and investigation of its anti-lung cancer effects, *Arab. J. Chem.* 14, 2021,103224.
- Sree, N.V., Udayasri, P., Suresh, V., Rao, K.R.S.S., 2009. Osteoporosis: Use of Nanoparticles for the Treatment of Osteoporosis. *Biomed. Pharmacol. J.* 2 (2), 477–488.
- Timmersmans, S., Souffriau, J., Libert, C., 2019. A General Introduction to Glucocorticoid Biology. *Front. Immunol.* 10, 1545.
- Umamaheswari, C., Lakshmanan, A., Nagarajan, N.S., 2018. Green synthesis, characterization and catalytic degradation studies of gold nanoparticles against congo red and methyl orange. *J. Photochem. Photobiol. B* 178, 33–39.
- Van Staa, T.P., Leufkens, H.G.M., Abenhaim, L., Zhang, B., Cooper, C., 2000. Use of oral corticosteroids and risk of fractures. *J. Bone Miner. Res.* 15 (6), 993–1000.
- Veisi, H., Ozturk, T., Karmakar, B., Tamoradi, T., Hemmati, S., 2020. In situ decorated Pd NPs on chitosan-encapsulated Fe₃O₄/SiO₂-NH₂ as magnetic catalyst in Suzuki-Miyaura coupling and 4-nitrophenol reduction. *Carbohydr. Polym.* 235, 115966.
- Venditti, I., 2019. Engineered gold-based nanomaterials: morphologies and functionalities in biomedical applications. A mini review, *Bioengineering* 6 (2), 53–78.
- L. Xu, Y.-Yi Wang, J. Huang, C. Y. Chen, Z. -X. Wang, H. Xie, Silver nanoparticles: Synthesis, medical applications and biosafety, *Theranostics* 2020; 10(20):8996-9031.
- Xu, J., Li, L., Zhang, J., Min, Y., 2021. Decorated of Au NPs over L-arginine-modified Fe₃O₄ nanoparticles as a novel nanomagnetic composite for the treatment of human ovarian cancer. *Arab. J. Chem.* 14, (7) 103283.
- W. Xue, G. Yang, B. Karmakar, Y. Gao, Sustainable synthesis of Cu NPs decorated on pectin modified Fe₃O₄ nanocomposite: Catalytic synthesis of 1-substituted-1H-tetrazoles and in-vitro studies on its cytotoxicity and anti-colorectal adenocarcinoma effects on HT-29 cell lines, *Arab. J. Chem.* 14, 2021,103306.
- Yin, I.X., Zhang, J., Zhao, I.S., Mei, M.L., Li, Q., Chu, C.H., 2020. The Antibacterial Mechanism of Silver Nanoparticles and Its Application in Dentistry. *Int J Nanomedicine.* 15, 2555–2562.
- Zhang, W., Veisi, H., Sharifi, R., Salamat, D., Karmakar, B., et al, 2020. Fabrication of Pd NPs on pectin-modified Fe₃O₄ NPs: A magnetically retrievable nanocatalyst for efficient C-C and C-N cross coupling reactions and an investigation of its cardiovascular protective effects. *Int. J. Biol. Macromol.* 160, 1252–1262.
- Zhao, P., El-kott, A., Ahmed, A.E., Khames, A., Zein, M.A., 2021. Green synthesis of gold nanoparticles (Au NPs) using *Tribulus terrestris* extract: Investigation of its catalytic activity in the oxidation of sulfides to sulfoxides and study of its anti-acute leukemia activity. *Inorg. Chem. Commun.* 131, 108781.